

Trapped-hole centers associated with trivalent cations in tetragonal GeO₂

R. B. Bossoli, T. J. Welsh, and O. R. Gilliam
*Department of Physics and Institute of Materials Science,
 University of Connecticut, Storrs, Connecticut 06268*

M. Stapelbroek*

Naval Research Laboratory, Washington, D.C. 20375

(Received 8 August 1978)

X-ray irradiation at 77 K of single crystals of tetragonal GeO₂ containing Sc³⁺, Y³⁺, and In³⁺ substitutional impurities generates trapped-hole centers analogous to the [Al]⁰ and [Ga]⁰ centers reported previously in Al-doped and Ga-doped crystals. The spin-Hamiltonian parameters for the [Sc]⁰ center are: $g_x = 2.0276 \pm 0.0004$, $g_y = 2.0115 \pm 0.0004$, $g_z = 2.0039 \pm 0.0004$, $|A_x| = 4.70 \pm 0.20$, $|A_y| = 4.39 \pm 0.20$, and $|A_z| = 4.64 \pm 0.20$. For [Y]⁰ the parameters are: $g_x = 2.0340 \pm 0.0004$, $g_y = 2.0112 \pm 0.0004$, $g_z = 2.0040 \pm 0.0004$, $|A_x| = 1.42 \pm 0.20$, $|A_y| = 1.64 \pm 0.20$, and $|A_z| = 1.40 \pm 0.20$, where the A tensor components are in units of 10^{-4}cm^{-1} . From symmetry, the only contribution to the isotropic part of the hyperfine interaction for the [Sc]⁰ and [Y]⁰ centers is due to exchange core polarization. The result that the core-polarization parameter is negative for [Sc]⁰ centers and positive for [Y]⁰ centers is found consistent with previously reported [Al]⁰ centers with negative- and [Ga]⁰ centers with positive-core-polarization parameters. Differences in [Y]⁰-center annealing properties and cation site occupation compared to the other neutral centers is presumed related to an ionic size effect introducing distortions into the GeO₂ lattice.

I. INTRODUCTION

Trapped-hole centers, where the hole is trapped on an O²⁻ ion adjacent to a charge-deficient cation site, have been reported in numerous metal oxides. A variety of vacancy-associated (V centers)¹ and impurity-related (e.g., [Li]⁰ and [Na]⁰)² trapped-hole centers have been well characterized in the alkaline-earth oxides. An indication of the extensive interest in trapped-hole centers can be gained from a recent review by Weil³ of the Al-associated centers in α -quartz which listed 125 references! Numerous other centers consisting of holes trapped on O²⁻ anions adjacent to charge-deficient cation sites have been observed in other oxide materials including Al₂O₃,⁴ YAlO₃,⁵ ZnO,^{6,7} and SrTiO₃.⁸

We have previously reported trapped-hole centers which occur following irradiation in tetragonal GeO₂ containing Al or Ga impurities.^{9,10} These centers were labeled the [Al]⁰ and [Ga]⁰ centers and consist of a hole trapped on one of the four equivalent (out of six) near-neighbor O²⁻ ions adjacent to a substitutional Al³⁺ or Ga³⁺ impurity cation. Here we present results on the similar [Sc]⁰ and [Y]⁰ centers and compare these with the [Al]⁰ and [Ga]⁰ centers. Observation of an analogous center in In-doped material is

also reported; however, precise parameters were not obtained for this center because of the complexity of the electron-spin-resonance (ESR) spectrum. Results for the [X]⁰ centers (with X = Al, Sc, Ga, or Y) in tetragonal GeO₂ will be compared with the recently reported Al-associated trapped-hole centers in TiO₂,^{11,12} and SnO₂,^{13,14} and Ga-associated centers in SnO₂.^{13,14}

II. EXPERIMENTAL DETAILS

The doped single crystals of tetragonal GeO₂ were obtained by slow cooling a GeO₂-Na₂O flux doped with approximately 400 ppm of the impurity ion in the form of Sc₂O₃, Y₂O₃, or In₂O₃. The trapped-hole centers were usually generated by x irradiation at liquid nitrogen temperature; however, they were also produced by ⁶⁰Co- γ -ray or uv irradiation at this temperature.⁹ ESR measurements were made on Varian E-3 and E-12 X-band spectrometers at 92 K. Precise alignment of the crystals was obtained using a Laue x-ray backscattering technique.

At 92 K the resonance lines for all of these centers were less than 0.5 G wide and began to saturate with less than 1 mW of microwave power.

III. RESULTS

The ESR spectra for the $[X]^0$ centers and the In-associated center in tetragonal GeO_2 for \vec{H} parallel to the crystallographic $[001]$ direction (the c axis) are shown in Fig. 1. For this orientation, all defect sites are equivalent and the characteristic hyperfine patterns are evident for some of these centers. Forbid-

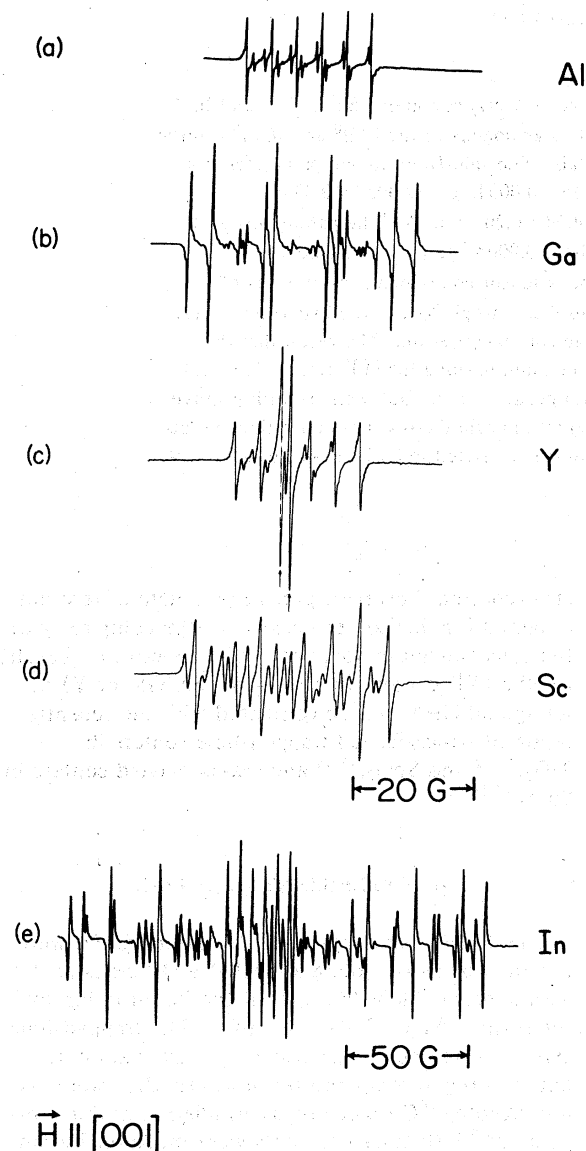


FIG. 1. ESR first-derivative spectra measured at 9.2 GHz and 92 K with $\vec{H} \parallel \vec{c}$ for all $[X]^0$ centers and for the In-associated center. The dopant impurity cation is labeled on the right for each spectrum. Figures 1(a) through 1(c) have the same sweep rate as Fig. 1(d); for all figures the magnetic field increases to the right. In Fig. 1(c) a weaker $[Al]^0$ background spectrum is evident in addition to the hyperfine doublet of the $[Y]^0$ center.

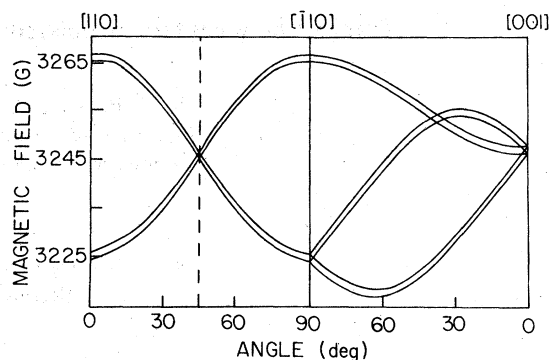


FIG. 2. Angular dependence of ESR lines of $[Y]^0$ centers in tetragonal GeO_2 for magnetic field variation in the (001) and (110) planes.

den hyperfine transitions, which have been analyzed for the $[Al]^0$ center,¹⁵ become so prominent in the spectra of $[Sc]^0$ and In-associated centers that the hyperfine patterns for allowed transitions tend to be obscured. Table I lists relevant isotopic properties for the impurity nuclei. The ESR angular dependence for the $[Y]^0$ center is shown in Fig. 2, where magnetic field variation is in the (001) and (110) planes. Similar plots are obtained for the other $[X]^0$ centers (excluding differences due to hyperfine interactions).

Figure 3 is a plot of the relative ESR absorption for individual $[X]^0$ centers as a function of temperature for isochronal pulse anneals. For these measurements samples were x-irradiated at 77 K and the ESR signals measured at 92 K without warm-up. Samples were annealed for five minutes at each temperature, and brought back to 92 K for measurement of the ESR signal intensity. The results show that, with the exception of the $[Y]^0$ center, all of the $[X]^0$ centers and the In-associated center begin to decay at about 120 K and are completely annealed by 170 K. The $[Y]^0$ centers, however, are more stable and do not begin to decay until 150 K, and do not disappear un-

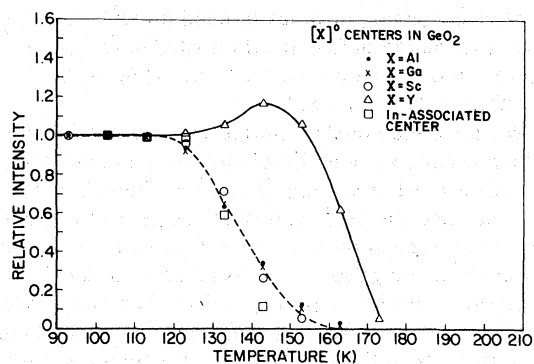


FIG. 3. Temperature dependence of the $[X]^0$ centers and the In-associated center measured using 5-min isochronal pulse anneals.

TABLE I. Isotopic properties and ionic radii for trivalent impurity cations.

Isotope ^a	Percent Abundance	Nuclear Spin	Nuclear Moment (Units of μ_N)	X^{3+} Radius ^b (\AA)
²⁷ Al	100	$\frac{5}{2}$	3.6385	0.530
⁴⁵ Sc	100	$\frac{7}{2}$	4.7492	0.730
⁶⁹ Ga	60.4	$\frac{3}{2}$	2.011	0.620
⁷¹ Ga	39.6	$\frac{3}{2}$	2.5549	0.620
⁸⁹ Y	100	$\frac{1}{2}$	-0.13682	0.892
¹¹⁵ In	95.72	$\frac{9}{2}$	5.5079	0.790

^aIsotopic data obtained from Ref. 16.

^bEffective ionic radii for sixfold coordination based on $r[\text{O}^{2-}] = 1.40 \text{ \AA}$ (Ref. 18).

til about 180 K. In fact an approximately 20% growth in the $[\text{Y}]^0$ centers has been detected for an anneal near 145 K (see Fig. 3), which is believed to be associated with the decay of $[\text{Al}]^0$ centers that are also present in these crystals. The growth of $[\text{Y}]^0$ is more prominent in samples that have received x-ray doses sufficiently small that the $[\text{Y}]^0$ centers are not growth saturated. This enhancement of the $[\text{Y}]^0$ ESR signal when the $[\text{Al}]^0$ centers decay, strongly suggests that the $[\text{Al}]^0$ centers and the other $[\text{X}]^0$ centers decay by a hole-release process and not by recombination with electrons released from some unknown trap in the crystals. Similar results have been observed for the V^- centers which grow at the expense of the V_{OH} centers in MgO .¹⁷ We have, however, no definitive explanation for the extra stability exhibited by the $[\text{Y}]^0$ centers. The Y^{3+} ion's large radius, compared to the radius of the Ge^{4+} ion that it replaces, would cause a larger distortion of the nearby lattice than the other X^{3+} impurity cations, which might contribute to a higher thermal stability. Ionic radii of the impurity cations are shown in Table I; the radius of the Ge^{4+} cation is 0.540 \AA .¹⁸ An attempt to detect $[\text{Yb}]^0$ centers using similar experimental procedures was not successful; the ionic radius of Yb^{3+} [0.93 \AA] (Ref. 18) is presumed too large to be accommodated by the GeO_2 crystal lattice.

IV. THE MODEL

The model we have adopted for the $[\text{X}]^0$ centers in tetragonal GeO_2 is illustrated in Fig. 4. In the following paragraphs we show that this model is consistent with all experimental results. All $[\text{X}]^0$ centers are described by the spin Hamiltonian

$$\mathcal{H} = \mu_B \vec{S} \cdot \vec{g} \cdot \vec{H} + \vec{S} \cdot \vec{A} \cdot \vec{I} + \vec{I} \cdot \vec{Q} \cdot \vec{I} - g_N \mu_N \vec{H} \cdot \vec{I}, \quad (1)$$

where the symbols have their usual meanings. For an arbitrary orientation of the magnetic field, up to four magnetically inequivalent sites can be observed. This is reduced to three for \vec{H} in the (110) or $(\bar{1}\bar{1}0)$ planes, two for \vec{H} in the (001) plane, and only one for \vec{H} in the (100) and (010) planes. These inequivalencies are in accord with the model, as discussed in Ref. 9. In the remainder of the paper, comments will be with respect to that magnetically inequivalent site illustrated by Fig. 4.

The point symmetry at the trapped-hole site is

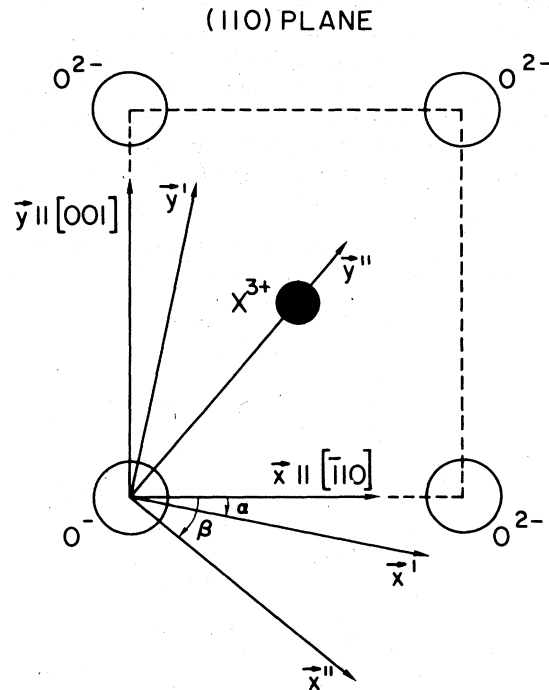


FIG. 4. Model for $[\text{X}]^0$ centers in tetragonal GeO_2 .

TABLE II. Comparison of principal g values and angles α , defined in Fig. 4, for impurity-related trapped-hole centers in tetragonal TiO_2 , GeO_2 , and SnO_2 crystals.

	g_x	g_y	g_z	α	Ref.
GeO ₂ :					
[Al] ⁰	2.0202 ± 0.0002	2.0143 ± 0.0002	2.0040 ± 0.0002	11.6° ± 0.5°	9
[Ga] ⁰	2.0249 ± 0.0003	2.0132 ± 0.0003	2.0039 ± 0.0003	19.4° ± 0.5°	10
[Sc] ⁰	2.0276 ± 0.0004	2.0115 ± 0.0004	2.0039 ± 0.0004	27° ± 3°	This
[Y] ⁰	2.0340 ± 0.0004	2.0112 ± 0.0004	2.0040 ± 0.0004	27° ± 3°	work
SnO ₂ :Al	2.0229 ± 0.0005	2.0196 ± 0.0005	2.0059 ± 0.0005	0°	12,13
SnO ₂ :Ga	2.0217 ± 0.0005	2.0228 ± 0.0005	2.0049 ± 0.0005	0°	14
TiO ₂ :Al (I)	2.0192 ± 0.0005	2.0261 ± 0.0005	2.0034 ± 0.0005	26°	11

monoclinic (C_s), the only two symmetry elements being the identity and reflection through the (110) plane. By symmetry, therefore, \bar{g} , \bar{A} , and \bar{Q} must have one common principal axis perpendicular to the reflection plane¹⁹ (the \bar{z} axis) along the [110] direction. The other principal axes of these tensors are not constrained by symmetry.

The nearly-free-electron principal value of the \bar{g} tensor also occurs along the \bar{z} -axis direction, indicating that the hole is trapped in the $2p_z$ nonbonding orbital of the oxygen anion. This has been confirmed by an ab-initio point-ion crystal-field calculation⁹ for the [Al]⁰ center, and this conclusion is applicable to all of the $[X]^{0}$ centers. Furthermore, the value of α [defined in Fig. 4] for the [Al]⁰ center that is predicted from the calculation is in close agreement with the measured value. The calculated g shifts are too large by about a factor of 2. However, such a discrepancy is not unreasonable since the calculations neglect the effects of lattice distortion, covalency, ion

size, and polarization effects.⁹ Principal g values and the angle α measured for the $[X]^{0}$ centers in GeO_2 are listed in Table II, along with results for similar centers in TiO_2 and SnO_2 .

Principal axes for the hyperfine tensor are also constrained by the model. In addition to the orientation of the \bar{z} axis which is required by symmetry, a principal axis is expected to occur along the $X^{3+}-O^{-}$ bond direction and the third axis must, of course, be orthogonal to these. A detailed analysis of the hyperfine interaction, including a first-principles calculation of the anisotropic part, was performed for the [Al]⁰ and [Ga]⁰ centers.¹⁰ It was determined from symmetry that the only contribution to the isotropic part of the hyperfine interaction is due to exchange core polarization. Table III lists experimental values of the hyperfine tensor, with signs determined by comparison with calculations, and gives the angle β [indicated in Fig. 4] determined for each of the $[X]^{0}$ centers.

TABLE III. Comparison of principal values of \bar{A} (in units of 10^{-4} cm^{-1}) and angles β , defined in Fig. 4, for impurity-associated trapped-hole centers in structurally similar crystal lattices.

	A_x	A_y	A_z	β	Ref.
GeO ₂ :					
[Al] ⁰	-4.50 ± 0.05	-3.57 ± 0.05	-4.51 ± 0.05	36.6° ± 1.0°	9
[⁶⁹ Ga] ⁰	9.13 ± 0.03	10.27 ± 0.05	9.62 ± 0.05	36° ± 2°	10
[⁷¹ Ga] ⁰	11.49 ± 0.05	12.89 ± 0.05	11.85 ± 0.05	36° ± 2°	10
[Sc] ⁰	-4.70 ± 0.2	-4.39 ± 0.2	-4.64 ± 0.2	27° ± 3°	This
[Y] ⁰	-1.42 ± 0.2	-1.64 ± 0.2	-1.40 ± 0.2	27° ± 3°	work
SnO ₂ :Al	2.59	3.53	3.56		12,13
SnO ₂ :Ga	7.10	6.70	7.00		14
TiO ₂ :Al (I)	5.99	4.97	5.99	36° ± 3°	11

V. DISCUSSION

Because the X^{3+} nucleus lies in the nodal plane of the $2p_z$ oxygen orbital containing the unpaired spin, overlap of X^{3+} core s orbitals with the $2p_z$ O^- orbital vanishes. Therefore, unpaired spin density due to overlap and covalency effects is not expected at the impurity ion's nucleus. The isotropic part of the hyperfine interaction for the $[X]^0$ centers can therefore be attributed to exchange core polarization.¹⁰ This mechanism has previously been proposed for the isotropic hyperfine interaction of $[Li]^0$ centers in ZnO and BeO,²⁰ and for $[Li]^0$ and $[Na]^0$ centers in MgO, CaO, and SrO.²

The core-polarization parameter χ which represents the difference between the density of spin-up (+) (parallel to unpaired spin) and spin-down (-) electrons at the nucleus is defined as²¹

$$\chi \equiv \frac{4\pi}{2S} \sum_i [|\phi_i^+(O)|^2 - |\phi_i^-(O)|^2], \quad (2)$$

where $S = \frac{1}{2}$ and i ranges over all the core s orbitals of the impurity ion. The parameter χ was determined for the $[Y]^0$ and $[Sc]^0$ centers from the formula

$$a_0 = \frac{2}{3} g_e \mu_B g_N \mu_N \chi \quad (3)$$

which represents the core-polarization contribution to the Fermi-contact hyperfine interaction. The results for $[Sc]^0$ and $[Y]^0$ centers are listed in Table IV along with those for $[Al]^0$ and $[Ga]^0$ centers.

A two-step mechanism for core polarization in the $[Ga]^0$ center was advanced to explain the difference in the sign of χ between the $[Al]^0$ and $[Ga]^0$ centers.¹⁰ Because the exchange interaction acts like an attractive interaction,²² the unpaired spin in the $2p_z$ oxygen orbital would tend to cause an outward relaxation of the (+)-spin-impurity-cation s orbitals resulting in a negative contribution to χ . For the heavier impurity ions (e.g., Ga^{3+} and Y^{3+}), outward relaxation of the outer-shell (+)-spin s electrons could result in inward relaxation of the inner-shell (+) electrons, giving a positive contribution to χ .

TABLE IV. Core-polarization parameters of $[X]^0$ centers in tetragonal GeO_2 .

Center	χ	Ref.
$[Al]^0$	-0.136	10
$[^{71}Ga]^0$	0.334	10
$[Sc]^0$	-0.292	This
$[Y]^0$	0.255	work

The new results presented here are consistent with this mechanism.

An interesting phenomenon was also observed in some crystals doped with yttrium. As for the other $[X]^0$ centers, Y^{3+} enters the lattice substitutionally for Ge^{4+} in either of the two cation sites in the unit cell. These two sites are chemically equivalent, however, and are related to each other by a 90° rotation about the c axis. As can be seen in the ESR spectrum shown in Fig. 5, an order-of-magnitude difference exists in the Y^{3+} population of these two cation sites for this sample. Similar effects have been observed for Al^{3+} impurities in α -quartz.²³ The difference in population of the two sites was found to vary from sample to sample, but few samples were found to have the expected equal amount of Y^{3+} in both sites. These effects may be due to long-range strains in the crystal (caused by the large ionic radius of Y^{3+}) which result in the preferential incorporation of Y^{3+} impurity ions into one of the two cation sites during crystal growth.

The $[X]^0$ centers in GeO_2 are significantly different from the trapped-hole centers in SnO_2 . For $SnO_2:Al$ the hole at low temperatures is localized on one of the two equivalent (\bar{a})-type oxygen anions,¹³ and not on one of the four equivalent closer (\bar{b})-type anions, which trap the holes in GeO_2 . [See Fig. 1 in Ref. 9 depicting (\bar{a}) and (\bar{b}) sites]. In addition, above 115 K motional effects are observed which are attributed to the hole's hopping between the two equivalent (\bar{a}) anions. For the trapped-hole center in $SnO_2:Ga$ experimental results at 40 K are interpreted by assum-

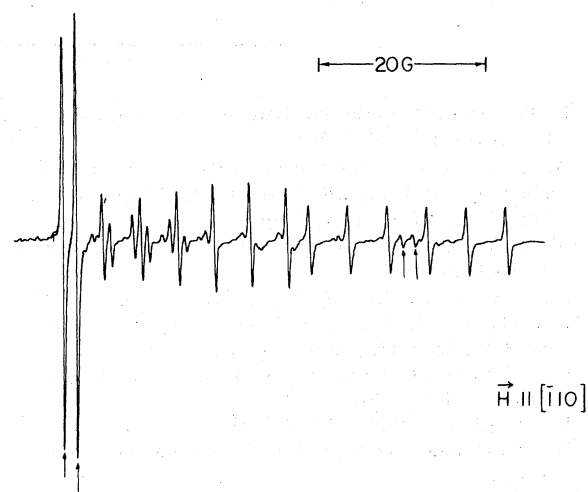


FIG. 5. ESR spectrum showing unequal site population of $[Y]^0$ centers in two inequivalent cation sites in tetragonal GeO_2 . The $[Y]^0$ centers give rise to hyperfine doublets indicated by the arrows. The other resonance lines result from $[Al]^0$ centers (six-line hyperfine patterns and forbidden transitions) for which the cation site populations are approximately equal.

ing hole-hopping between (\bar{b}) anions. Such motional effects were not observed for any of the $[X]^0$ centers in GeO_2 . Excluding the $[\text{Y}]^0$ center, at temperatures higher than 120 K, where motional effects might be expected, the $[X]^0$ centers have annealed.

Three different Al-related paramagnetic trapped-hole centers have been reported¹¹ in tetragonal TiO_2 (rutile). Irradiation with uv of Al-doped rutile at 10 K produced a center that has been reported analogous to the $[\text{Al}]^0$ center in GeO_2 ; i.e., a hole trapped on one of the four (\bar{b}) anions. Two other centers, which appeared somewhat above 30 K were attributed to more complex defect structures.¹¹

In the anatase phase of TiO_2 a radiation-induced trapped-hole center associated with a substitutional Al^{3+} impurity cation exhibits a striking resemblance to the $[\text{Al}]^0$ center in tetragonal GeO_2 .¹² This arises for each of these two crystal structures since there are four magnetically inequivalent oxygen sites having approximately the same orientation with respect to the crystallographic axes. The point symmetry at the O^- site is C_s in both materials. There is only a difference in the $\text{Al}^{3+}\text{-O}^-$ bond directions, which are 40° and 80° from the c axis in tetragonal GeO_2 and anatase, respectively. This results in a substantially different orientation of the hyperfine tensor principal axes in the two cases.^{9,12}

VI. SUMMARY

Three new trapped-hole centers, $[\text{Sc}]^0$, $[\text{Y}]^0$, and an In-associated center, have been observed in tetragonal GeO_2 by ESR at 92 K after x-irradiation at

liquid-nitrogen temperature. Results for the $[\text{Y}]^0$ and $[\text{Sc}]^0$ centers are similar to those found for the $[\text{Al}]^0$ and $[\text{Ga}]^0$ centers in GeO_2 , SnO_2 , and TiO_2 , and have been explained by a model consisting of a hole trapped in a nonbonding p orbital of one of the four (out of six) near-neighbor oxygen anions adjacent to the Sc^{3+} or Y^{3+} impurity ion. The thermal stabilities of the $[X]^0$ centers indicate that they decay via a hole-release mechanism and not by recombination with electrons released from other traps in the crystal.

The core-polarization parameters for the $[\text{Sc}]^0$ and $[\text{Y}]^0$ centers, which were obtained from the observed isotropic part of the hyperfine interaction, have sign variations consistent with those previously reported for the $[\text{Al}]^0$ and $[\text{Ga}]^0$ centers. However, for the $[\text{Y}]^0$ center, compared to the other $[X]^0$ centers, differences were observed in the hole-annealing behavior and in the impurity-cation site occupation of the Y^{3+} ions.

ACKNOWLEDGMENTS

We wish to thank Linda Wagner for her assistance on the experimental measurements for the $[\text{Sc}]^0$ center and Dr. E. Kostiner for advice on crystal preparation. The computational portions of this investigation were performed at the University of Connecticut Computer Center. This work was supported by a grant from the University of Connecticut Research Foundation and by a National Research Council fellowship to M. Stapelbroek at the Naval Research Laboratory.

*Present Address: Electronic Systems Group Rockwell Int., Anaheim, Calif. 92803

- ¹A. E. Hughes and B. Henderson, in *Point Defects in Solids*, edited by J. H. Crawford, Jr. and L. M. Slifkin (Plenum, New York, 1972), Vol. I, Chap. 7.
- ²M. M. Abraham, W. P. Unruh, and Y. Chen, *Phys. Rev. B* **10**, 3540 (1974).
- ³J. A. Weil, *Radiat. Eff.* **16**, 261 (1975).
- ⁴F. T. Gamble, R. H. Bartram, C. G. Young, O. R. Gilliam, and P. W. Levy, *Phys. Rev.* **134**, A589 (1964).
- ⁵O. F. Schirmer, K. W. Blazey, W. Berlinger, and R. Diehl, *Phys. Rev. B* **11**, 4201 (1975).
- ⁶D. Zwingel, *J. Lumin.* **5**, 385 (1972).
- ⁷D. Zwingel and F. Gartner, *Solid State Commun.* **14**, 45 (1974).
- ⁸O. F. Schirmer, W. Berlinger and K. A. Muller, *Solid State Commun.* **18**, 1505 (1976).
- ⁹M. Stapelbroek, R. H. Bartram, O. R. Gilliam, and D. P. Madacsi, *Phys. Rev. B* **13**, 1960 (1976).
- ¹⁰M. Stapelbroek, O. R. Gilliam, and R. H. Bartram, *Phys. Rev. B* **16**, 37 (1977).
- ¹¹D. Zwingel, *Solid State Commun.* **20**, 397 (1976).
- ¹²V. S. Grunin, G. D. Davtyan, V. A. Ioffe, and I. B.

Patrina, *Phys. Status Solidi B* **77**, 85 (1976).

- ¹³D. Zwingel, *Phys. Status Solidi B* **77**, 171 (1976).
- ¹⁴E. Mollwo and D. Zwingel, *J. Lumin.* **12/13**, 441 (1976).
- ¹⁵M. Stapelbroek, R. H. Bartram and O. R. Gilliam, *Phys. Rev. B* **16**, 4737 (1977).
- ¹⁶*Handbook of Chemistry and Physics*, 53rd ed. (Chemical Rubber, Cleveland, 1972), p. E-57.
- ¹⁷L. A. Kappers and J. E. Wertz, *Solid State Commun.* **9**, 1755 (1971).
- ¹⁸R. D. Shannon and C. T. Prewitt, *Acta Crystallogr. B* **25**, 925 (1969).
- ¹⁹G. E. Pake and T. L. Estle, *The Physical Principles of Electron Paramagnetic Resonance* (Benjamin, Reading, Mass., 1973).
- ²⁰O. F. Schirmer, *J. Phys. Chem. Solids* **29**, 1407 (1968).
- ²¹A. Abragam and B. Bleaney, *Electron Paramagnetic Resonance of Transition Ions* (Clarendon, Oxford, England, 1970), p. 697.
- ²²R. E. Watson and A. J. Freeman, in *Hyperfine Interactions*, edited by A. J. Freeman and R. B. Frankel (Academic, New York, 1967), p. 60.
- ²³J. H. Mackey, J. W. Boss, and D. E. Wood, *J. Magn. Res.* **3**, 44 (1970).